Heliyon 10 (2024) e28237

Contents lists available at ScienceDirect

Heliyon

journal homepage: www.cell.com/heliyon

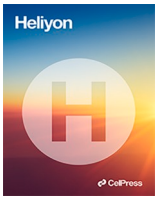

Research article

Prognostic insights and immune microenvironment delineation in acute myeloid leukemia by ferroptosis-derived signature

Lijun Jing [a], Biyu Zhang [b], Jinghui Sun [c], Jueping Feng [d], Denggang Fu [c,*]

[a] Department of Neurology, the First Affiliated Hospital of Zhengzhou University, Zhengzhou, 450052, China
[b] School of Chemical Engineering & Pharmacy, Wuhan Institute of Technology, Wuhan, 430205, China
[c] College of Medicine, Medical University of South Carolina, Charleston, SC, 29425, United States
[d] Department of Oncology, Wuhan Fourth Hospital, Wuhan, 430033, China

ARTICLE INFO

Keywords:
Acute myeloid leukemia
Cell death
Ferroptosis
Prognosis
Immune niche

ABSTRACT

Acute myeloid leukemia (AML) represents as a prevalent and formidable hematological malignancy, characterized by notably low 5-year survival rates. Ferroptosis has been found to be correlated with cancer initiation, therapeutic response, and clinical outcome. Nevertheless, the involvement of Ferroptosis-related genes (FRGs) in AML remains ambiguous. Five independent AML cohorts totaling 1,470 (GSE37642, GSE12417, GSE10358, Beat-AML, and TCGA-AML) patients with clinical information were used to systematically investigated the influence of these FRGs expression on outcome and tumor microenvironment. The integration of these datasets led to the subdivision into training and validation sets. Nineteen FRGs were identified as correlated with the overall survival (OS) of AML patients, primarily enriched in ferroptosis, fatty acid metabolism, and leukemia-related signaling pathways. The prognostic signature, consisting of 11 FRGs, was formulated using LASSO-Cox stepwise regression analysis. Patients with high-risk scores exhibited reduced survival compared to those in the low-risk group. The receiver operating characteristic (ROC) analysis underscored the signature's robust predictive accuracy. The high predictive efficacy was confirmed by both internal and external validation datasets. Leukemia and signaling related to immune regulation were mainly enriched pathways of the differentially expressed genes by comparing high- and low-risk groups. The immune composition deconvolution might indicate an immunosuppressive niche in the high-risk patients. The pRRophetic algorithm exploration unveiled chemical drugs with potentially sensitivity among patients in both groups. Collectively, our study developed a ferroptosis-derived prognostic signature that provides the OS prediction and identifies the immune microenvironment for AML patients on large-scale AML cohorts.

1. Introduction

Acute myeloid leukemia (AML) is a prevalent and lethally blood malignancy, marked by the immature myeloid cell accumulation in bone marrow and peripheral blood [1]. Patients with AML have a poor prognosis and a high relapse risk that are mostly attributed to therapeutic resistance to chemotherapy [2]. 5-year survival has been not greatly improved over several decades, and still listed as one of the lowest survivals among all blood cancers from 1975 to 2014 [3]. Therapeutic options for AML patients have not witnessed

* Corresponding author. 86 Jonathan Lucas St, Charleston, SC, 29425, United States.
E-mail address: fud@musc.edu (D. Fu).

https://doi.org/10.1016/j.heliyon.2024.e28237
Received 23 May 2023; Received in revised form 13 March 2024; Accepted 14 March 2024
Available online 15 March 2024

significant progress. The standard care for AML still revolves around chemotherapy, yet a considerable number of patients succumb to the disease primarily due to relapse. Molecular targeting therapies including FLT3 inhibitors [4], IDH and c-KIT inhibitors have made a remarkable leap forward. While gemtuzumab ozogamicin, targeting CD33-positive AML, has been utilized in the treatment of AML, its widespread use has been limited due to high toxicity. CAR T-cell therapy [5] and bi-specific antibodies that engage T cells with new antigens expressed on tumor cells [6] have emerged as novel, safe, and highly effective treatments for blood cancers, including AML. However, it's worth noting that most therapies based on these concepts are currently in various stages of preclinical or clinical trials. Therefore, it's crucial to uncover novel potential signatures to enhance patient prognosis monitoring and aid in the advancement of effective therapies.

Ferroptosis, a non-apoptotic, iron-dependent form of programmed cell death which is different from necroptosis, apoptosis, and autophagy [7], has been found to be associated with tumorigenesis, disease progression, and the response to drugs. It exerts diverse functions in biological processes and cellular signaling cascades [8–10]. Ferroptosis is characterized by redox-active iron levels, impaired repair of lipid peroxides, and oxidation of polyunsaturated fatty acids. Emerging research suggests that susceptibility to ferroptosis is influenced by factors like RAS/MAPK signaling, amino acid and iron metabolism, cell adhesion, phospholipid biosynthesis, p53 status, and the activity of NRF2 [11]. Numerous genes, validated to promote or inhibit ferroptosis, are referred as ferroptosis-related genes (FRGs) in tumor cells. Examples include G6PD, TP53 [12], GPX4 [13], SLC7A11 [14] and DHODH [15]. Previous studies demonstrated that ferroptosis represents promising anti-cancer therapeutic target [16–18]. Exposure to APR-246 can trigger ferroptosis-mediated anti-tumor activity in AML cells by augmenting cystine uptake, thus sustaining the synthesis of the antioxidant molecule glutathione [19]. The novel all-trans retinoic acid derivative, 4-amino-2-trifluoromethyl-phenyl retinate (ATPR), has showed potent anti-tumor activity in AML. ATPR triggers ferroptosis in AML cells by modulating autophagy through iron homeostasis, suggesting that directing ferroptosis enhances ATPR-induced AML differentiation via the ROS-autophagy-lysosomal signaling [20]. In their study, Hai-Yan Zhu et al. discovered that typhaneoside stimulates autophagy in AML cells by activating AMPK pathway. This process leads to ferritin degradation, subsequent ROS accumulation, and ultimately ferroptosis [21]. Furthermore, in their research, Weimin Wang et al. revealed that treatment with anti-PD-L1/anti-CTLA-4 activated $CD8^+$ T cells, thereby fostering ferroptosis through targeted lipid peroxidation in tumor cells. This mechanism significantly contributes to the anti-tumoral effectiveness of the treatment [22]. Therefore, Understanding the interplay between ferroptosis and the leukemia microenvironment holds the potential to lead to the creation of novel and effective anti-leukemia treatments for AML. However, the roles of most FRGs in AML have remained largely unknown. Several studies utilizing computational biology have explored the potential clinical relevance of FRGs in AML. Several ferroptosis-related gene signatures have been proposed as potential prognostic indicators or therapeutic target for AML, whereas most of these signatures were established on limited AML patients and lack comprehensive independent validation [23–25]. Furthermore, the impact of ferroptosis-related signatures on responsiveness to therapeutic drugs has rarely been assessed. Some studies attempted to assess the prognostic implications of the expression patterns of FRGs in AML [26] or focused on the influence of ferroptosis-related non-coding RNAs on patients' outcomes using TCGA-AML data. Signatures based on non-coding RNAs are challenging to verify due to the limitations of the detective approaches used in high throughput methods such as microarrays [27]. Comprehensive analysis of FRGs in AML based on large scale of AML cohorts from multiple centers has not been thoroughly explored. Construction and validation of an FRGs-based signature on such large cohorts, used for assessing the leukemia microenvironment and forecasting the prognosis, also need further investigation.

Motivated by these unexplored aspects, this study systematically profiled the ferroptosis-related gene signatures and clinicopathological characteristics of 1,470 AML patients in Gene Expression Omnibus (GEO) (GSE37642, GSE12417, GSE31580), Beat-AML, and the Cancer Genome Atlas (TCGA) databases. The datasets underwent strategic division into a training set, internal validation set, and external validation sets. The prognostic relevance of these FRGs in AML was established via univariate Cox regression analysis. Subsequently, we crafted a robust ferroptosis-derived prognostic signature using Lasso-Cox regression analysis. Validation of the signature's predictive efficacy occurred across internal and three external validation sets, affirming its role as an effective indicator for monitoring AML patient outcomes. The study further delved into the leukemia immune microenvironment landscape delineated by the signature. Additionally, we investigated patients' responsiveness to therapies. Our findings offer innovative perspectives for developing new therapies targeting ferroptosis in AML.

2. Methods and materials

2.1. Data acquisitions and preprocessing

We obtained gene expression profiles and clinical data from the GEO and TCGA databases. Subsequently, we downloaded five AML cohorts containing relevant clinical information for subsequent analysis (GSE36732-GPL96, GSE36732-GPL570, GSE12417-GPL96, GSE12417-GPL570, GSE10358-GPL570, BeatAML, and TCGA-AML, Table S1). For Affymetrix® microarray data, we acquired raw "CEL" files and applied a robust multiarray averaging method using the affy packages to perform background adjustment and quantile normalization. Probe IDs were transferred to gene symbols using platform annotated packages, and in cases where a gene had multiple probes, the average value was adopted. For different datasets measured by the same platform, we eliminated batch effects stemming from non-biological sources using the combat algorithm via the sva package [28]. The RNA-sequencing data for TCGA-AML was retrieved from UCSC Xena database (https://xenabrowser.net/datapages/).

2.2. Discovery of FRGs associated with overall survival (OS)

Samples measured by the GPL96 platform from GSE37642 and GSE12417 were amalgamated, followed by random and equitable allocation into training (n = 290) and internal validation (n = 290) sets. From the FerrDb database, we extracted a comprehensive collection of 159 experimentally validated FRGs, classified into drivers, suppressors, and markers [29] (http://www.zhounan.org/ferrdb/, Table S2). The expression matrix of 132 FRGs were extracted across these AML datasets. OS-related FRGs were identified through univariate Cox regression analysis, considering significance at $p < 0.05$.

2.3. Development and validation of a prognostic signature derived from ferroptosis

To mitigate the potential overfitting, feature selection was conducted to identify OS-related FRGs using multivariate lasso-cox regression analysis. The optimal signature's minimum features were determined using the Akaike information criterion [30]. The discrimination ability of the model was evaluated by the receiver operating characteristic curve (ROC) with survivalROC package. Individual patient's risk scores were computed by multiplying the gene expression value of the model by the corresponding coefficient. Subsequently, patients were stratified into low- and high-risk groups using the median risk score as the cutoff. The predictive performance of the signature was assessed using log rank test with "survminer" package and illustrated using Kaplan-Meier curve.

The prognostic performance was verified by internal validation set (n = 290) and external three independent cohorts (samples measured by GPL570 from GSE37642, GSE10358 and GSE12417; Beat-AML; TCGA-AML).

The heterogenous AML populations in our work should be noted as they may receive various therapeutical regimens. Univariate and multivariate Cox regression analyses assessed the prognostic independence of the prognostic signature by incorporating accessible clinicopathological factors. Accessible features from the training and validation sets were collected. The information on age, the French-American-British (FAB) classifications, and RUNX1/RUNX1T1 fusion was only available from the training and internal validation datasets. Gender, age, FAB classifications, and ELN2017 were available in TCGA-AML dataset. In addition, the information on gender, ELN2017, FLT3_ITD, NPM1 mutation, WBC count, BM blast, PB blast, and platelet count was obtainable from Beat-AML validation set.

2.4. Identification and functional analysis of DEGs between low- and high-risk groups

DEGs with |LogFC| greater than 0.5 and adjust p value less than 0.05 were screened by comparing high- and low-risk groups through "limma" [31]. Gene enrichment analysis, covering biological process (BP), molecular function (MF), and cellular components (CC), was conducted with clusterProfiler [32]. KEGG pathway analysis was conducted, with a significance threshold set at p value less than 0.05.

Furthermore, to reveal the potential enriched pathways of these DEGs, gene set enrichment analysis (GSEA) was performed [33]. Genes were ranked based on their significance in the annotated "C2:KEGG gene sets" between low- and high-risk groups. The significant gene set, determined through 1000 permutations, had a p-value <0.05.

2.5. Tumor immune microenvironment (TIME) analysis

The tumor niche comprises the tumor and its surrounding microenvironment, including immune cells, stromal cells, signaling molecules, and extracellular matrix. We employed the CIBERSORT algorithm [34] to assess the infiltration of 22 immune cell types in both high- and low-risk groups, characterizing the composition of immune cells based on gene expression data mixture. A total of 7 types of T cells, naïve and memory B cells, plasma cells, and NK cells are included. The cases with $p < 0.05$ were delivered for further analysis.

In addition, the expression of PD-1, CTLA-4, CD33, and CD123 between high- and low-risk groups were compared using Wilcox test, with statistical significance set at $p < 0.05$.

2.6. Construction of ferroptosis-derived clinicopathologic nomogram

A ferroptosis-derived clinicopathologic nomogram was developed to predict OS for each AML patient. This included patient risk score along with available clinicopathologic parameters from the training set using rms package [35]. A calibration curve was plotted to assess the predictive performance [36].

2.7. Chemotherapeutic response prediction

Given that chemotherapy is the mainstream clinical regime for treating AML, the prediction of potential chemicals responsive to AML was performed based on the IC50 value using the pRRophetic package [37] according to the GDSC database [38]. This methodology involved constructing statistical models from gene expression and drug sensitivity data across a broad panel of cancer cell lines. These models were then applied to gene expression data obtained from primary tumor biopsies.

3. Results

3.1. Identification and enrichment analysis of OS-related FRGs in AML

In order to determine clinical relevance of FRGs in AML, Nineteen FRGs significantly correlated with patient outcomes were identified via univariate Cox regression analysis in training set (Fig. 1A). The FRGs network illustrated the comprehensive landscape of interactions, regulator connection, and prognostic significance for AML patients (Fig. 1B). To investigate underlying functions of the FRGs in AML, GO terms exploration suggested that these FRGs were primarily involved in metabolic and biosynthetic associated biological processes including fatty acid biosynthesis and metabolism, iron ion binding (Fig. 1C). Ferroptosis, PPAR, AMPK, autophagy, and mTOR signaling pathways were the predominantly signaling pathways (Fig. 1D). These pathways are vital in disease development and served as therapeutic targets in hematological malignancies including AML [39–42]. This suggests a crucial role for these FRGs in AML progression, promoting further investigation into their relationship with the tumor microenvironment.

3.2. Development and validation of a ferroptosis-derived prognostic signature

To prevent overfitting, the minimum key survival-related FRGs were assessed by Lasso regression (Figs. S1A–B). A prognostic ferroptosis-derived signature was developed via multivariate Cox stepwise regression. The final optimal signature of 11 genes was determined using AIC algorithm within the "survival" package (Fig. 2A). Ferroptosis-derived risk score (named as FerroScore) for an individual patient was calculated as following formula:

$$\text{FerroScore} = \sum_{i}^{n} Coef \text{ x } A_i$$

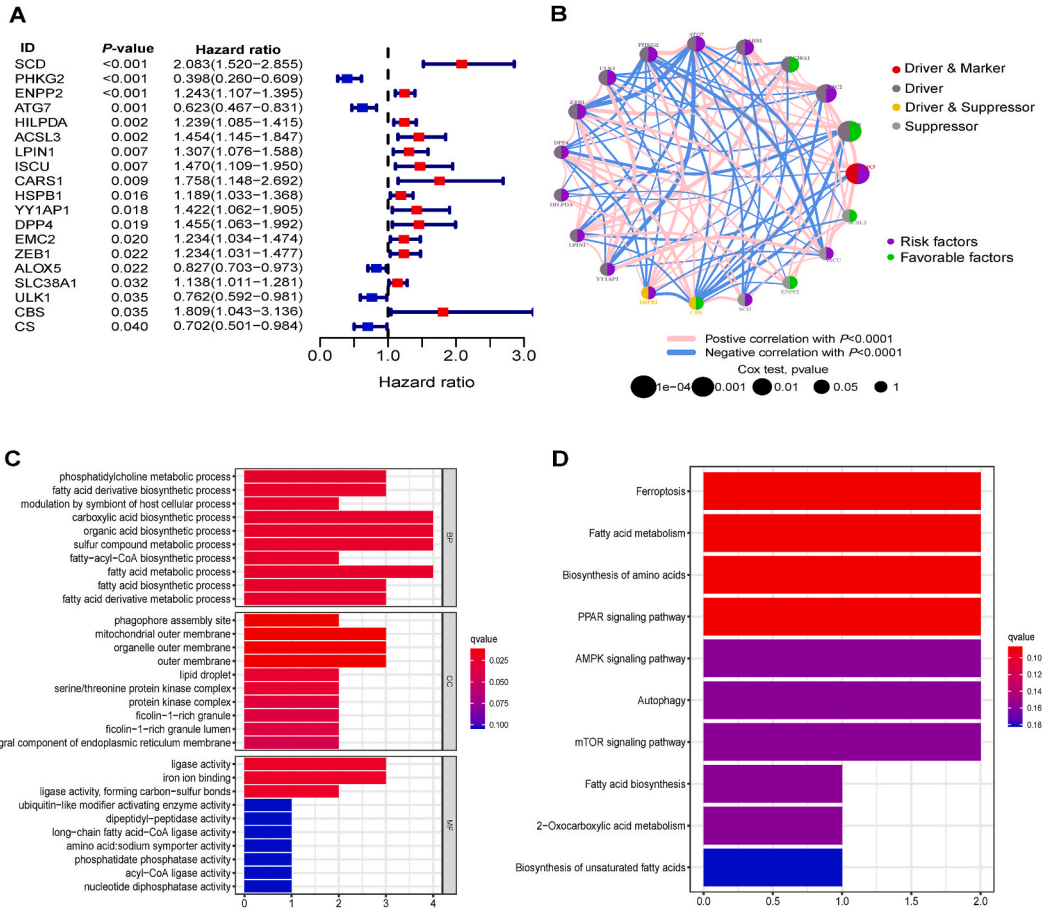

Fig. 1. Clinical relevance of the FRGs in AML (A). Prognostic FRGs in AML. (B). The interplay among FRGs in AML. The circle size represents regular effect for the prognosis, and p-values calculated by Log-rank test was $p < 1e\text{-}4$, $p < 1e\text{-}3$, $p < 0.01$, and $p < 0.05$, respectively. Purple dots, risk factors of outcomes; Green dots, protective factors of outcomes. Lines indicate regulator interactions, with thickness reflecting correlation strength. Blue and red colors show negative and positive correlations. (C–D). GO terms analysis and pathways of prognostic FRGs. (For interpretation of the references to color in this figure legend, the reader is referred to the Web version of this article.)

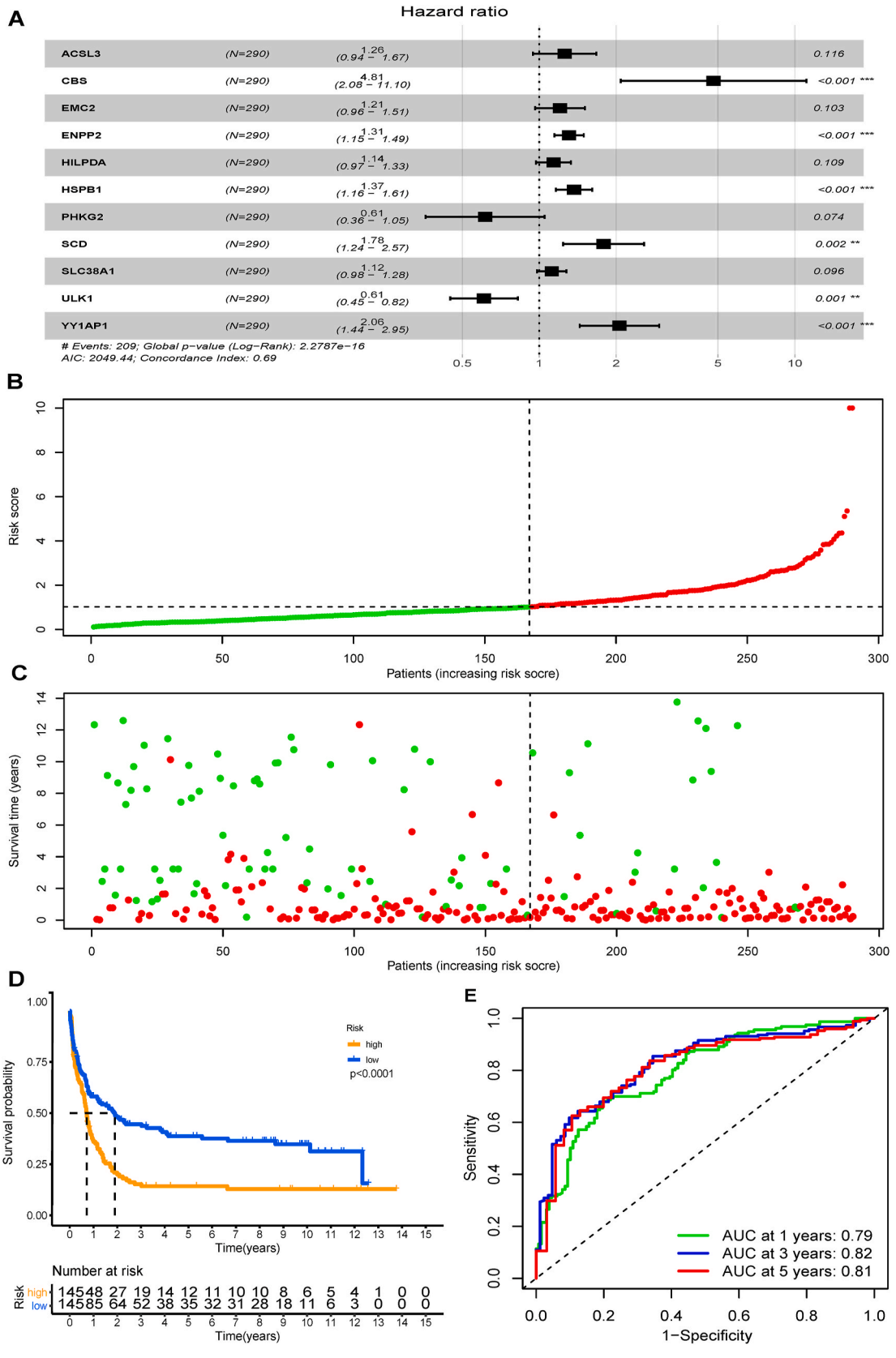

(caption on next page)

Fig. 2. Generation of a ferroptosis-derived prognostic signature in AML (A). Signature's features. (B). Range of patients' risk scores. (C). Survival time plotted against risk scores. (D). High-risk group has decreased OS. (E). ROC curves for 1-, 3, and 5-year in the training set.

In this equation, "Coef" stands for the regression coefficient, "i" represents the signature gene, "A" represents the relative value of the signature expression, and "n" represents the number of signature genes.

Patients were categorized into high- and low-risk groups using the median risk score as the cutoff value. The number of deaths increased as the risk score rose (Fig. 2B–C). To dictate the predictive capacity of the prognostic signature, we generated a Kaplan-Meier curve revealing that patients in the low-risk group have better survival than those patients in the high-risk group ($P < 0.0001$, Fig. 2D). The predictive accuracy of the signature was appraised, yielding an AUC value of 0.82 for 3-year OS. Additionally, the AUCs for 1- and 5-year OS were 0.79 and 0.81, respectively, implying that accurate prognosis prediction efficiency (Fig. 2E). Furthermore, an internal

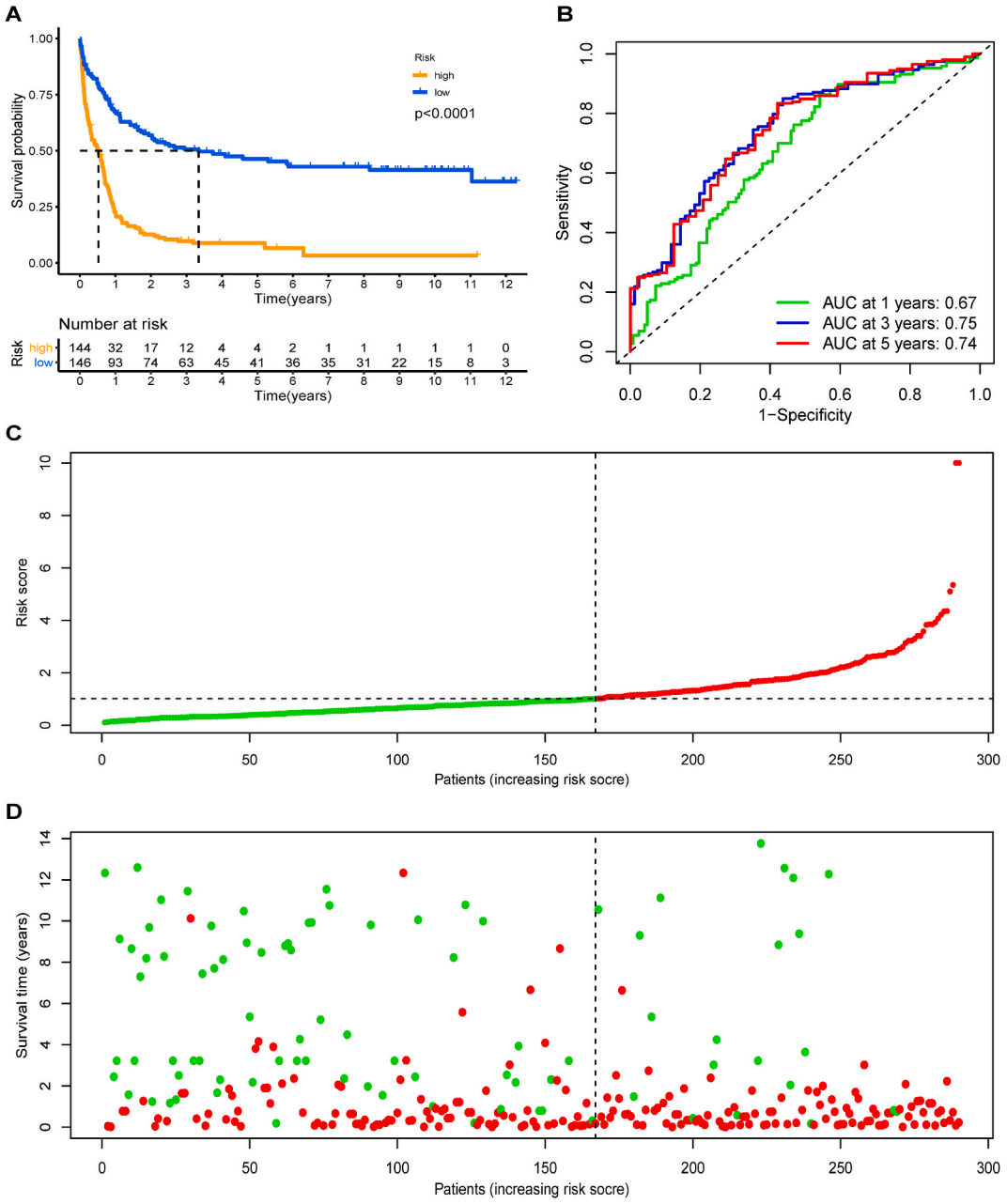

Fig. 3. Validation of the ferroptosis-derived signature in internal AML cohort (A). Patients with high-risk scores have decreased OS. (B). ROC curves for 1-, 3, and 5-year. (C). The Patients' risk scores. (D). Decreasing survival with increasing risk score.

validation set was used to verify its predictive reliability. Patients with high-risk scores also have decreased OS than those patients with low-risk scores ($P < 0.0001$, Fig. 3A). The AUCs of the signature in internal validation set were comparable to those in training set (Fig. 3B), the AUCs of 1-, 3-, and 5-year OS were 0.67, 0.75, and 0.74. As the risk score rose, so did the number of deaths (Fig. 3C–D). This indicates that the OS prediction of our signature was robust.

Additionally, as illustrated in Figs. S1C–D, the signature remained independent of accessible variables, including age, FAB classifications, and RUNX1/RUNX1T1 fusion, in the training and internal validation datasets using univariate and multivariate analysis. This suggests that the signature is an independent prognostic indicator for AML. Further interrogation by including more available

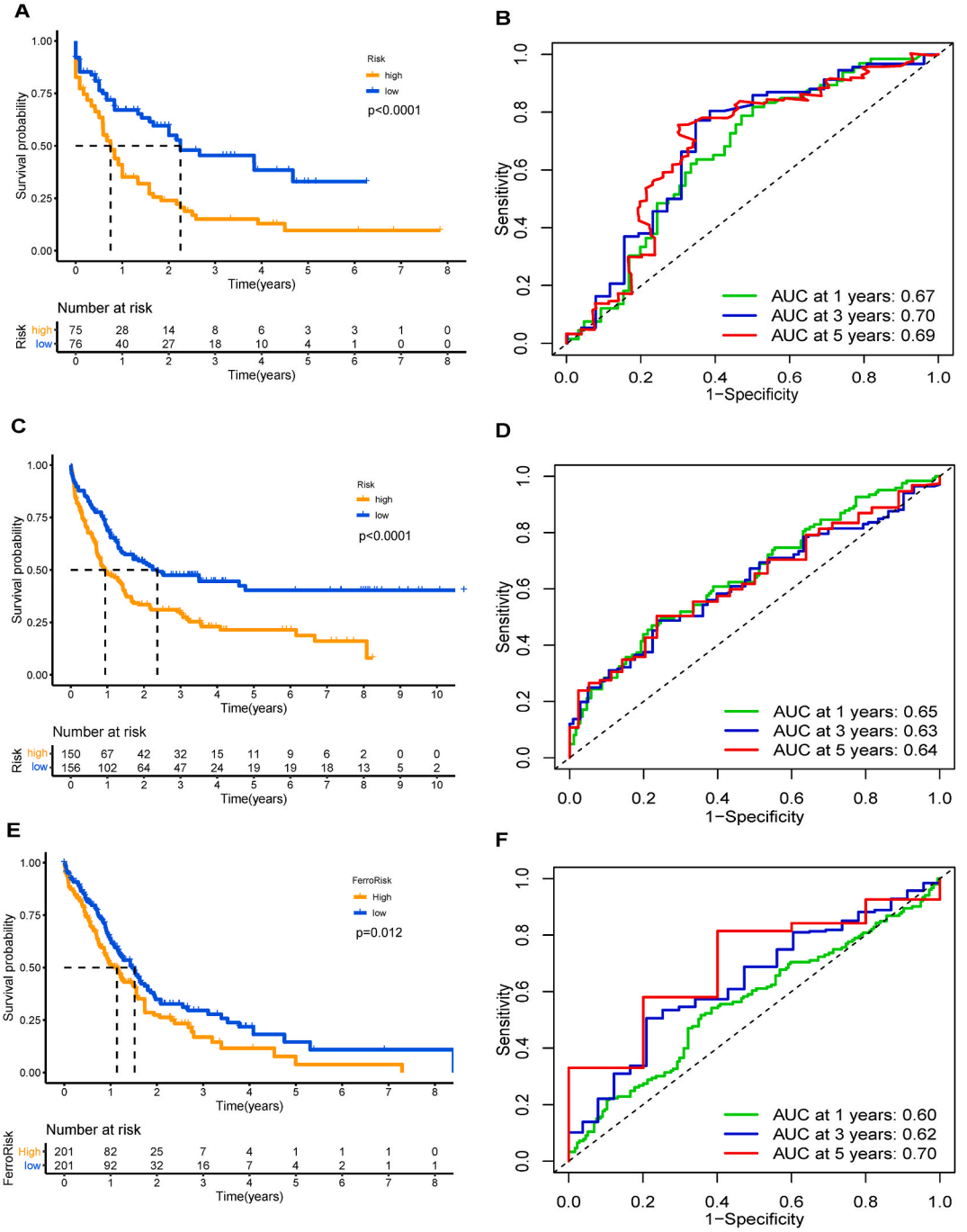

Fig. 4. Validation of the Ferroptosis-derived signature in external AML cohort (A). Patients with high-risk scores have decreased OS in TCGA-AML. (B). ROC curves for 1-, 3, and 5-year in TCGA-AML. (C). Decreased OS in combined AML samples from GPL570 platform. (D). ROC curves for 1-, 3, and 5-year in GPL570 platform AML. (E). High-risk group has decreased OS in Beat-AML. (F). ROC curves for 1-, 3, and 5-year in Beat-AML.

clinical factors including gender, age, ELN2017, FLT3-ITD and NPM1 mutation, and the risk score maintains its autonomy as a reliable predictor in TCGA-AML dataset, but it didn't reach significance (p = 0.092) by multivariate analysis (Table S3). This may be induced by the heterogeneity of the AML cohorts as they may receive different treatments before measuring gene expression profiles. Subset analysis was not feasible due to the insufficient number patients under each clinical feature, such as TP53 mutation status and different treatment schemes. It will be more convincing if more subsets of patients become available for future validation.

Three external datasets (TCGA-AML; GPL570 platform from GSE37642, GSE10358, and GSE12417; Beat-AML) were employed to validate the signature's forecast stability and independence for AML. Each patient's risk score, delineated by the signature, categorized them into high- and low-risk cohorts. Within the TCGA-AML cohort, individuals in the low-risk category experienced significantly prolonged overall survival compared to those in the high-risk group ($P < 0.0001$, Fig. 4A). Predictive accuracy of the signature in TCGA-AML was comparable to performance in the training set, and the AUC for predicting OS at three years stood at 0.70 (Fig. 4B). Similar remarkable survival stratifications were also observed in the combined cohort from the affy-GPL570 platform ($P < 0.0001$, Fig. 3C) and Beat-AML dataset ($P = 0.012$ Fig. 4E). ROC analysis showed these two validation sets had moderate capacity of OS prediction for AML patients (Fig. 4D–F). On the whole, this finding highlight that the prognostic signature has robust prognostic stratification for AML patients on both array- and RNA-seq-based platforms. Further validation in clinical samples is warranted.

3.3. Gene enrichment analysis of DEGs

Exploring the potential molecular regulatory mechanisms characterized by the signature, we identified 70 DEGs between high- and low-risk group using limma package. Of these, 32 DEGs exhibited upregulation, while 38 DEGs showed downregulation (Fig. 5A). Notably, distinct gene expression patterns were discernible in both groups (Fig. 5B). Functional analysis revealed that these DEGs predominantly participate in biological processes related to neutrophil-mediated immunity, leukocyte activity, and inflammatory response. Additionally, cellular components implicated include those found in the lumen, granule, and lysosome, such as secretory

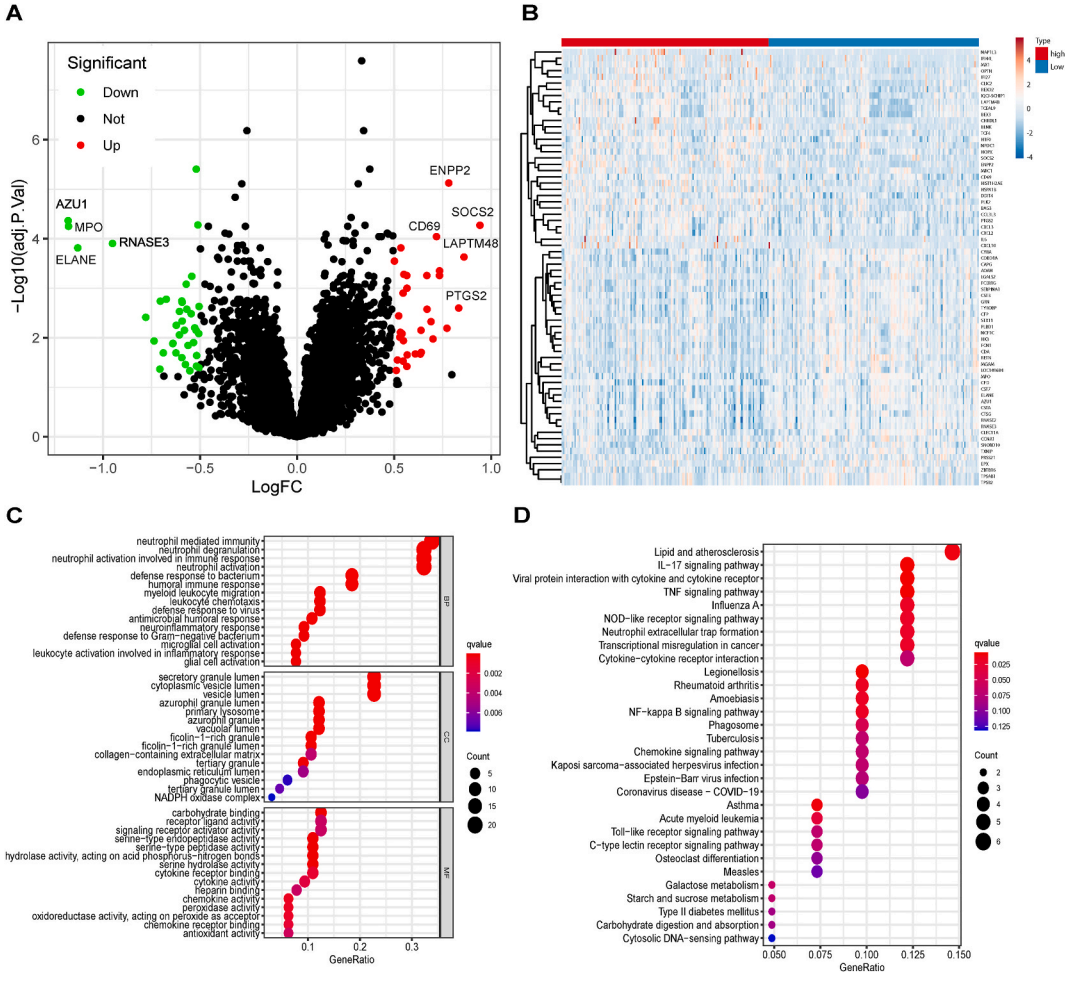

Fig. 5. Gene enrichment analysis of DEGs between high- and low-risk groups (A). Volcano plot. (B). Heatmap. (C). GO terms analysis. (D). KEGG pathways analyses.

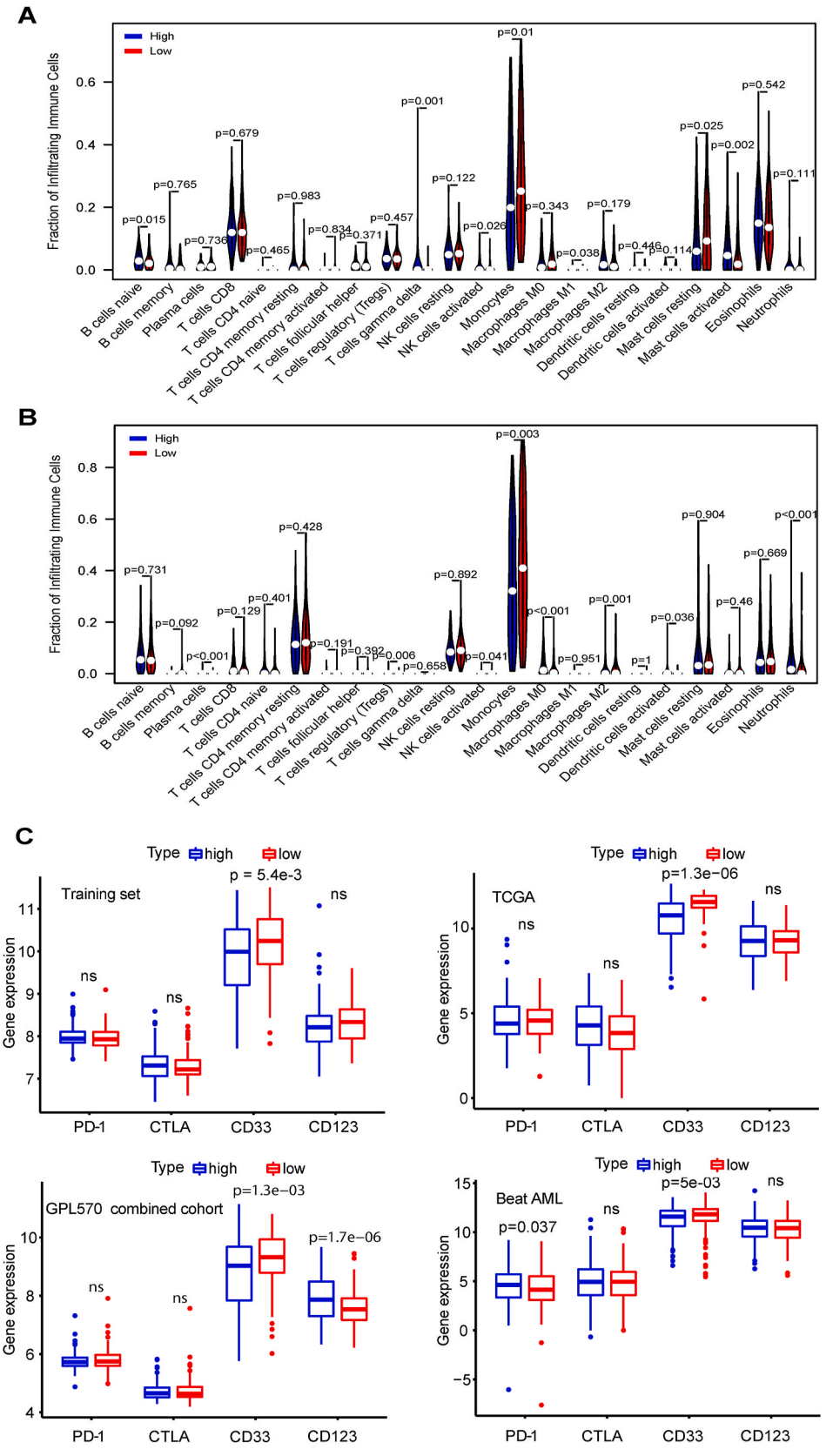

(caption on next page)

Fig. 6. Leukemic immune microenvironment analysis (A–B) The proportions of immune cells in high- and low-risk groups in the training and Beat-AML validation sets. (C). Immune checkpoints and targeted genes expression in training and validation sets.

granule lumen and cytoplasmic vesicle lumen. Molecular functions associated with serine hydrolase and peptidase activity, as well as cytokine and chemokine-related activities, were also identified (Fig. 5C). Furthermore, enriched pathways among these DEGs encompassed acute myeloid leukemia, IL-17, TNF, NF-Kappa B, chemokine, and cytokine-cytokine receptor interaction pathways

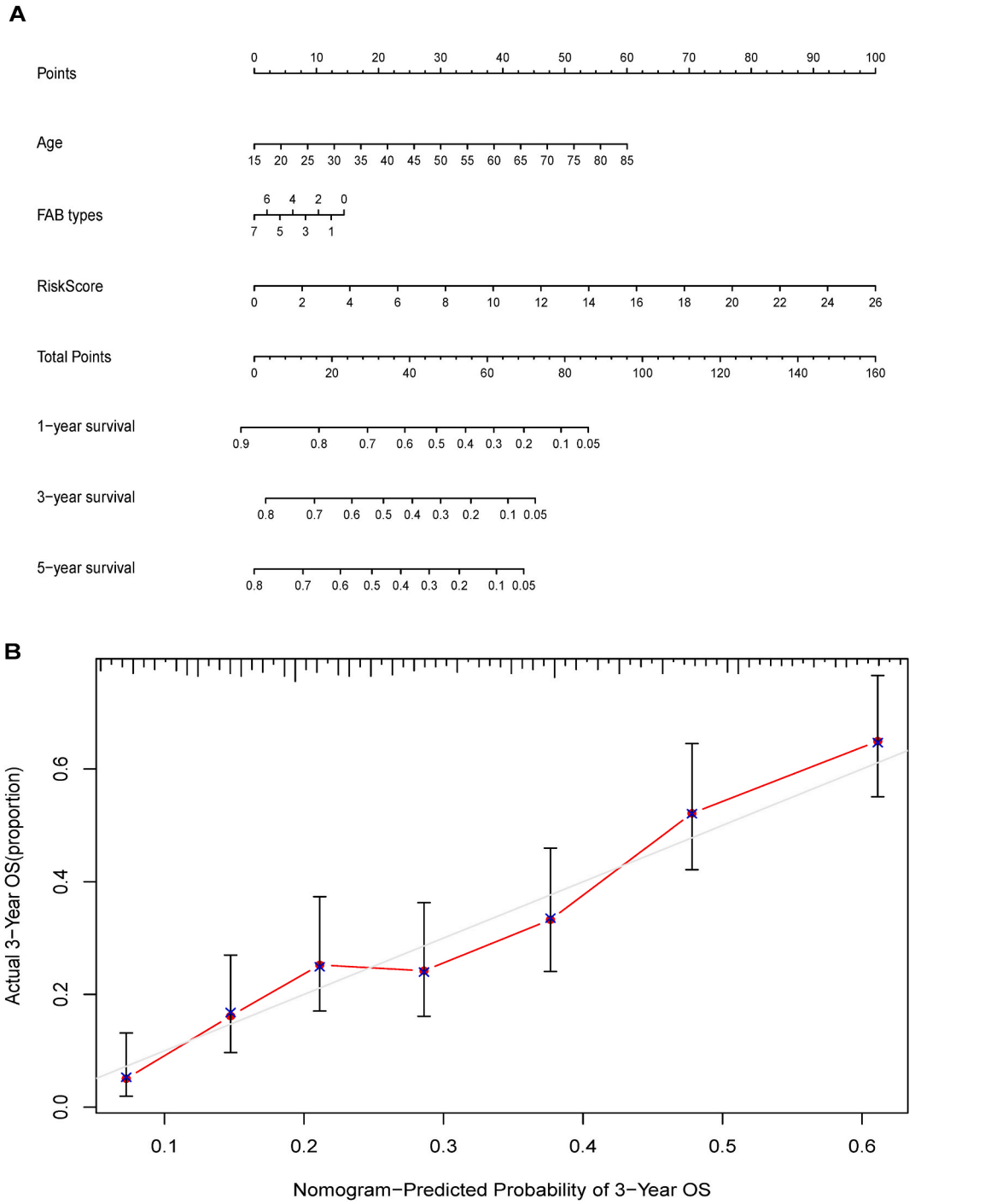

Fig. 7. Proposed predictive nomogram for AML (A). Ferroptosis-derived clinicopathologic nomogram for 1-, 3-, and 5-year OS monitoring for AML patients with risk score, age, FAB types. (B). Calibration curve for the probability of 3-year OS.

(Fig. 5D). Noteworthy, we observed that autophagy-related genes, such as BAG3 and SERPINA1, previously identified as potential prognostic factors for AML patients [43], were among the listed DEGs, suggesting a potential interplay between autophagy and ferroptosis in AML development. Moreover, we also identified the differentially expressed BLNK gene as a potential prognostic indicator in our recent work [44]. Research into the involvement of autophagy in ferroptosis has been explored and reviewed in various cancers, and enhanced autophagy contributes to ferroptosis through increasing the accumulation of intracellular iron levels [45].

GSEA revealed that the active involvement of these DEGs in lipid and acid-related metabolic pathways, glycosaminoglycan

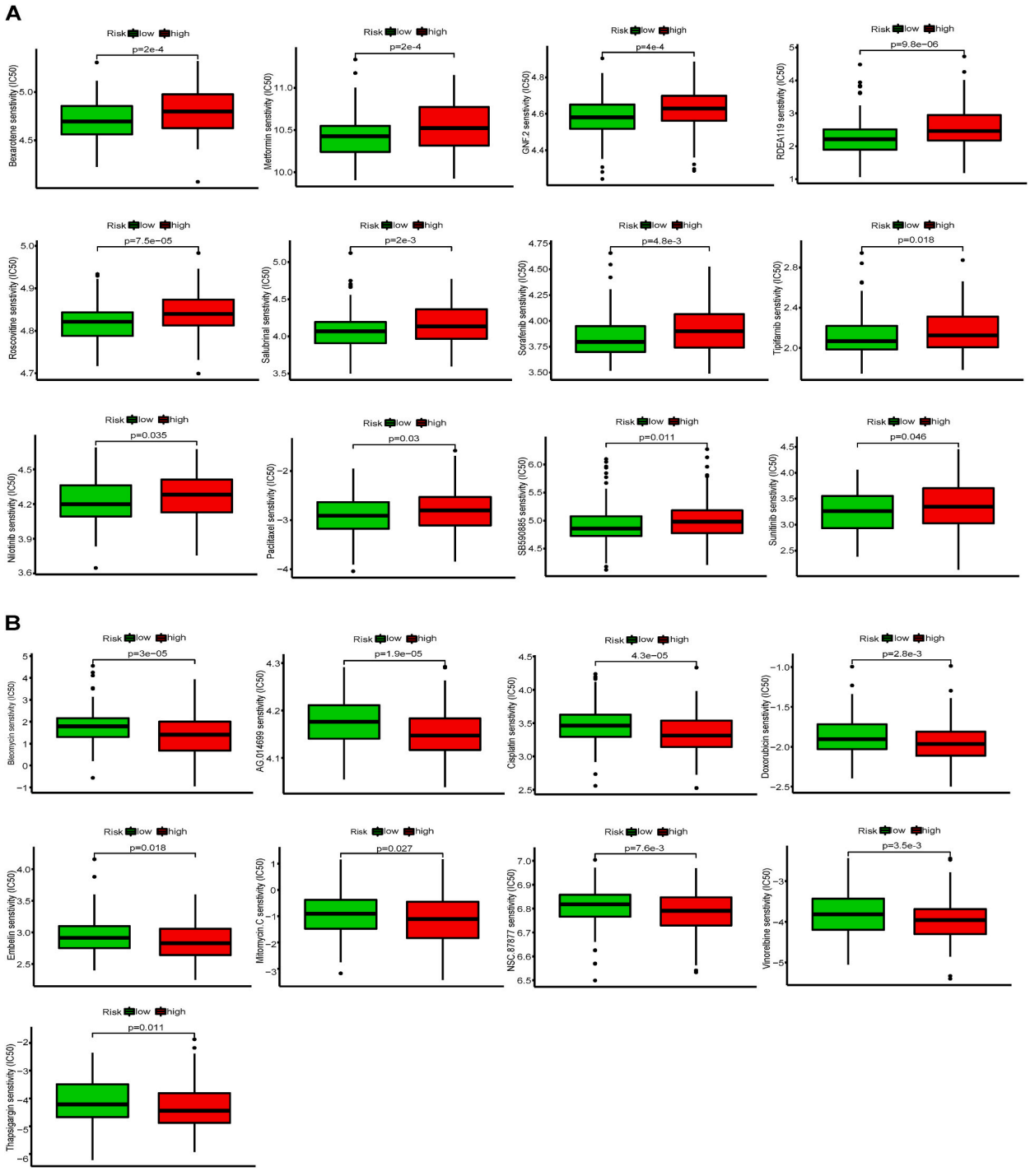

Fig. 8. Chemotherapeutic Response for AML patients (A). Potential drugs sensitive to low-risk patients. (B). Potential drugs sensitive to high-risk patients. IC50, half-maximal inhibitory concentration.

degradation and steroid biosynthesis (Figs. S2A–D). As a hallmark of ferroptosis, lipid peroxidation occurring in polyunsaturated fatty acid in the cell membrane can induce ferroptosis, and various lipid metabolic pathways have been reported to be engaged in ferroptosis [45,46]. These data insinuated that the DEGs discriminated by ferroptosis-derived signature might play important roles in AML progression, indirectly suggesting ferroptosis, emerging as a novel form of iron-dependent regulated cell demise marked by lipid peroxidation buildup, stands as a pivotal orchestrator in acute leukemia disease and immunity.

3.4. Characterization of TIME and implications for therapies through ferroptosis-derived signature

Given the implication of the ferroptosis-derived signature in immune regulatory signaling pathways within AML, coupled with the established influence of the TIME, notably tumor infiltrating lymphocytes (TILs), on both disease advancement and clinical outcome determinations. Twenty-two infiltrated immune cell types were deconvoluted using CIBESORT algorithm in both the training and Beat-AML validation datasets. Increased infiltrating gamma delta T cells (γδ T cells), activated NK cells, regulatory T cells (Tregs), M1 macrophages, and activated mast cells were observed in patients with high-risk scores, while high infiltrating monocytes and resting mast cells were noted in patients with low-risk scores (Fig. 6A–B). Among these cell types, γδ T cell was reported to promote angiogenesis and cell growth through production of IL-17 in the TIME [47] or increase numbers of myeloid derived suppressor cells [48]. TIME-derived Tregs show potent immunosuppressive activities than those from steady condition [49], and its infiltrates were elevated in patients with high-scores, revealing a suppressive TIME in patients from high-risk group.

Immunotherapy that represented by CART cells is a promising therapeutic strategy for refractory or relapsed AML patients [50]. High CD33 and CD123 have been found frequently express in AML blasts [51]. $CD33^{-}$and CD123-CART cell therapies have been demonstrated to be potent anti-leukemia activities *in vitro* and *in vivo assays* [52]. We found that CD33 is over-expressed in patients with low-risk scores across these AML cohorts, suggesting anti-CD33 CAR might be a potential immunotherapeutic option for low-risk AML patients (Fig. 6C). Furthermore, immune checkpoints blockade was widely employed to treat cancers including AML, while no significant difference in PD-1 and CTLA4 expression between high vs low-risk groups (Fig. 6C), even increased PD-1 expression was detected in low-risk patients in Beat-AML cohort. This indicated that ferroptosis-based signature might be relevant to immunotherapy in AML, but further work needs to be done for this hypothesis.

3.5. Construction of ferroptosis-derived clinicopathologic nomogram

Furthermore, to individually predict patients' outcome, the ferroptosis-derived prognostic signature was combined with available clinical parameters, including age and French-American-British Classifications, to develop a nomogram [53]. This, providing the survival probability at a specific time for patients, incorporated signature' score as a factor to assess the utility of OS prediction for 1-, 3-, and 5-year (Fig. 7A). Of note, cautious consideration should be taken to interpret this nomogram because it was built based on the limited known variables of AML patients, more prognostic variants included such as cytogenetics mutations will convince its clinical potential in the future. Additionally, a calibration curve of OS at 3 years were selected to illustrate the observed rates against the nomogram-predicted probabilities (Fig. 7B).

3.6. Chemotherapeutic response prediction for AML

Chemotherapy was still used as standard care for AML patients [2]. We performed chemotherapeutic response analysis using pRRophetic algorithm to predict the effective potential chemical drugs based on the IC50 data from GDSC database for patients. The estimated IC50 for each chemical or drug between high- and low-risk patients was analyzed, and we noted that both groups significantly sensitive to various chemical drugs, separately. 12 chemical drugs showed high sensitivity to low-risk patients (Fig. 8A), while low IC50 of 9 drugs were screened in high-risk patients (Fig. 8B). For example, low-risk patients exhibited enhanced sensitivity to Sorafenib and Roscovitine than that of high-risk patients. Sorafenib can prolong FLT3 mutated AML patients in relapse following allogeneic stem cell transplantation (allo-SCT) [54]. Preclinical data showed that Roscovitine, a cyclin-dependent kinase 2 inhibitor, arrests cell cycle and induces apoptosis in chronic lymphocytic leukemia [55], suggesting it might be an attractive drug for this incurable disease. Given that most patients with AML are resistant to chemotherapy after intensive induction and succumb to this disease. Further work is warranted to verify anti-leukemia efficacy of these drugs.

4. Discussion

Most effective anti-cancer therapies are aimed to selectively eliminate tumor cells with minimizing impairment to healthy cells [56]. Cell death including apoptosis, necrosis, pyroptosis, autophagy and oncosis has been identified in recent years. Cell death is critical to maintain biological homeostasis and disease advancement [57]. Increasingly recognized as a form of cell demise reliant on iron and lipid peroxidation, ferroptosis plays a dual role in tumorigenesis and anticancer therapies [56,58]. Ghoochani et al. showcased that ferroptosis inducers, like erastin or RSL3, alone or combined with second-generation antiandrogens, impede tumor cell proliferation and migration *in vitro*, as well as tumor expansion *in vivo*, suggesting a promising therapeutic avenue for advanced prostate cancer [59]. Additionally, Wang et al. illustrated that ferroptosis, orchestrated by $CD8^{+}$ T cells, impacts the effectiveness of cancer immunotherapy [22]. The involvement of ferroptosis in leukemia has attracted great attention, and several signatures designed to predict survival based on FRGs have been proposed. However, these signatures were developed on limited numbers of patients or lacked independent validation. Therefore, a systematical profiling of FRGs in AML remains unexplored. Understanding the ferroptosis

within acute myeloid leukemia microenvironment contributes to identify markers for monitoring prognosis and aiding in new therapeutic targets.

In this work, we first comprehensively investigated prognostic significance of FRGs in AML patients by integrating currently available AML datasets. To convince the validity of the study, only experimentally validated genes related with ferroptosis were obtained from FerrDb database. We found that 19 FRGs were correlated with patients' outcome. Correlation analysis showed potential distinct interactions among these survival related FRGs. In addition to ferroptosis, enriched pathways such as PPAR, AMPK, mTOR, and autophagy have been implicated in leukemia progression. This implies that ferroptosis probably has vital functions in AML. Identification specific FRG that has regulatory role in these signaling pathways needs to be investigated. We previously found autophagy-related genes including ULK1 are prognostic indicators [43,60]. This might be line with emerging research that ferroptosis is tightly associated with autophagy [61]. We established a robust prognostic classifier comprising 11 FRGs via Lasso-Cox regression model for monitoring patient survival. Patients that were stratified into the high-risk group have lower OS than those low-risk patients. 3-year AUC value was 0.82, indicating the signature has good predictive performance. The high stratification efficacy of our signature was independently validated by an internal and three external validation AML datasets, which indicates the present signature was robust and accurate across different cohorts and detection platforms. We noted that *Xianbo Huang* et al. recently proposed a 12-ferroptosis-derived signature to predict AML outcome, while sample size used for the training and validation was much smaller as compared to those in our study. Furthermore, predictive efficacy of the signature with few FRGs is comparable, which might make the signature more convincing. The signature stands alone as a predictor, even when adjusting for other clinical factors in both training and internal validation sets. In external validation datasets, we evaluated the prognostic signature's independence through univariate and multivariate regression analysis, incorporated clinical parameters like gender, age, and ELN2017 risk classifications, and found that risk score is a prognostic indicator after adjusting these features in TCGA-AML dataset, while it has prognostic effect but not reach significant level ($p = 0.092$) in Beat-AML dataset. The possible explanation is because they received multiple treatments before tumor biopsies, which leads AML patients heterogenous. In addition, the TP53 mutation status in this study was missing, we were not able to conduct the association analysis between the mutation and the signature. Further clinical subset validation will provide indicative clues for adjusting the signature.

TME has been demonstrated to affect patients' outcome and responsiveness to therapy. Therefore, to understand the influence of the ferroptosis-derived signature on the TME of AML, the infiltrating immune cell subsets were quantified using CIBERSORT algorithm, which might provide clues to delineate survival contrast in high- and low-risk patients. γδ T cells, activated NK cells, activated mast cells, and Treg cells were increased in patients with high-risk scores. In line with prior research, Treg cells can orchestrate immunosuppression within the TIME, facilitate to cancer immune evasion and lead to unfavorable outcome [62]. These tumor-infiltrating regulatory T cells possess diverse transcriptional states, which indicate their potential role in leukemia modulation [63]. Kai Yang et al. found that GPX4 guards against lipid peroxidation and ferroptosis to uphold Treg cell activation and inhibit anti-tumor activities [64], this inspires further investigation of FRG-expressing regulatory T cells in AML progression. γδ T cells have a dual function in cancer development. Non-MHC restricted recognition of antigens and high cytokine production of γδ T cells suggest it might be effective target in immunotherapies, while increased IL-17 secretion in tumor microenvironment can promote tumor growth [65]. On the other hand, high levels of MDSCs induced by γδ T cells also cause cancer development [48]. DEGs between high- and low-risk patients were predominantly involved in IL-17, cytokine-cytokine receptor interaction, chemokine, and NF-kappa B pathways. It might provide an explanation for patients within high-risk group have unfavorable survival. But it should be cautious to interpret γδ T cells function mediated by ferroptosis in AML due to γδ T cells can be classified into effector and regulatory γδ T cells have distinct functions [66]. Further investigation is warranted to clarify that the suppressive TME in high-risk groups is enhanced by regulatory γδ T cells.

The increasing benefits of immunotherapy for patients with various types of cancers including AML led to improved outcomes in recent years. No significant difference of immune checkpoint molecules like PD-1 and CTLA-4 expression between high- and low-risk patients. Interestingly, CD33 or CD123 were highly expressed in patients in low-risk patients, suggesting that they might respond to CD33-CART or CD123-CART cell therapies [52]. We also applied pRRophetic algorithm to screen potential effective chemicals for AML patients. The chemicals that showed distinct sensitivities to high- and low-risk patients were identified. Of these, several drugs were employed to treat leukemia patients. For example, Bleomycin has been approved by FDA to treat Hodgkin and non-Hodgkin lymphoma [67]. Doxorubicin was also FDA approved and indicated for the treatment of some types of blood cancers [68]. These drugs might have inhibitory efficacy for AML, and further verification is under the way.

This study established and verified a ferroptosis-based signature to predict outcomes for AML patients. However, there are limitations need to take into consideration. The FRGs were identified through experimental assays, necessitating validation of their roles in AML progression. The prognostic signature, validated using retrospective transcriptomic datasets, requires further confirmation of its robustness and accuracy in clinical utility. This includes validation at the proteomics level and in patients from multiple centers, considering the high heterogeneity of AML.

5. Conclusions

In this study, a ferroptosis signature was built and validated in both internal and three independent external AML datasets, allowing us to scrutinize distinct pathways, TIME, and therapeutic implications related to the signature. Further explorations of its clinical effectiveness and the molecular mechanisms of these FRGs in AML is imperative.

Ethical approval and informed consent

Human or animal experiments were not enrolled in the current study, and thus written consent is not required.

Data availability statement

The data used in this work are from the following databases.

1. TCGA: https://portal.gdc.cancer.gov/.
2. GEO: https://www.ncbi.nlm.nih.gov/geo/including GSE37642, GSE12417, and GSE10358.
3. UCSC Xena database: https://xenabrowser.net/datapages/.
4. Beat-AML: http://www.vizome.org/aml/.
5. STRING: https://string-db.org/cgi/input.pl.
6. FerrDb database: http://www.zhounan.org/ferrdb/.

Funding

Not applicable.

CRediT authorship contribution statement

Lijun Jing: Writing – original draft, Resources, Methodology, Formal analysis, Data curation. **Biyu Zhang:** Resources, Methodology, Formal analysis, Data curation. **Jinghui Sun:** Formal analysis, Data curation. **Jueping Feng:** Writing – review & editing. **Denggang Fu:** Writing – review & editing, Writing – original draft, Validation, Resources, Project administration, Data curation, Conceptualization.

Declaration of competing interest

The authors declare that they have no known competing financial interests or personal relationships that could have appeared to influence the work reported in this paper.

Acknowledgement

We extend our thanks to those who have contributed to public databases.

Abbreviations

AML	Acute myeloid leukemia
FRGs	Ferroptosis-derived genes
DEGs	differentially expressed genes
TME	Tumor microenvironment
CIBERSORT	Cell-type Identification By Estimating Relative Subsets Of RNA Transcripts
TILs	Tumor infiltrating lymphocytes
GEO	Gene Expression Omnibus
TCGA	The Cancer Genome Atlas
ICIs	Immune checkpoint inhibitors
PD-1	programmed cell death 1
CTLA-4	Cytotoxic T-lymphocyte-associated protein 4
GO	Gene Ontology
KEGG	Kyoto Encyclopedia of Genes and Genomes; OS, Overall survival

Appendix A. Supplementary data

Supplementary data to this article can be found online at https://doi.org/10.1016/j.heliyon.2024.e28237.

References

[1] D. Thomas, R. Majeti, Biology and relevance of human acute myeloid leukemia stem cells, Blood 129 (12) (2017) 1577–1585.
[2] L. Marando, B.J.P. Huntly, Molecular landscape of acute myeloid leukemia: prognostic and therapeutic implications, Curr. Oncol. Rep. 22 (6) (2020) 61.

[3] A. Jemal, E.M. Ward, C.J. Johnson, K.A. Cronin, J. Ma, B. Ryerson, et al., Annual report to the Nation on the status of cancer, 1975-2014, featuring survival, J. Natl. Cancer Inst. 109 (9) (2017).
[4] A.I. Antar, Z.K. Otrock, E. Jabbour, M. Mohty, A. Bazarbachi, FLT3 inhibitors in acute myeloid leukemia: ten frequently asked questions, Leukemia 34 (3) (2020) 682–696.
[5] S. Mardiana, S. Gill, CAR T cells for acute myeloid leukemia: State of the art and future directions, Front. Oncol. 10 (2020) 697.
[6] Q. Wang, Y. Chen, J. Park, X. Liu, Y. Hu, T. Wang, et al., Design and production of bispecific antibodies, Antibodies 8 (3) (2019).
[7] L. Galluzzi, I. Vitale, S.A. Aaronson, J.M. Abrams, D. Adam, P. Agostinis, et al., Molecular mechanisms of cell death: recommendations of the nomenclature committee on cell death 2018, Cell Death Differ. 25 (3) (2018) 486–541.
[8] Z. Shen, J. Song, B.C. Yung, Z. Zhou, A. Wu, X. Chen, Emerging strategies of cancer therapy based on ferroptosis, Adv. Mater. 30 (12) (2018) e1704007.
[9] B.R. Stockwell, J.P. Friedmann Angeli, H. Bayir, A.I. Bush, M. Conrad, S.J. Dixon, et al., Ferroptosis: a regulated cell death nexus linking metabolism, redox biology, and disease, Cell 171 (2) (2017) 273–285.
[10] B.R. Stockwell, X. Jiang, A physiological function for ferroptosis in tumor suppression by the immune system, Cell Metabol. 30 (1) (2019) 14–15.
[11] J. Li, F. Cao, H.L. Yin, Z.J. Huang, Z.T. Lin, N. Mao, et al., Ferroptosis: past, present and future, Cell Death Dis. 11 (2) (2020) 88.
[12] L. Jiang, N. Kon, T. Li, S.J. Wang, T. Su, H. Hibshoosh, et al., Ferroptosis as a p53-mediated activity during tumour suppression, Nature 520 (7545) (2015) 57–62.
[13] S. Ma, E.S. Henson, Y. Chen, S.B. Gibson, Ferroptosis is induced following siramesine and lapatinib treatment of breast cancer cells, Cell Death Dis. 7 (2016) e2307.
[14] S.J. Wang, D. Li, Y. Ou, L. Jiang, Y. Chen, Y. Zhao, et al., Acetylation is crucial for p53-mediated ferroptosis and tumor suppression, Cell Rep. 17 (2) (2016) 366–373.
[15] C. Mao, X. Liu, Y. Zhang, G. Lei, Y. Yan, H. Lee, et al., DHODH-mediated ferroptosis defence is a targetable vulnerability in cancer, Nature 593 (7860) (2021) 586–590.
[16] M.A. Badgley, D.M. Kremer, H.C. Maurer, K.E. DelGiorno, H.J. Lee, V. Purohit, et al., Cysteine depletion induces pancreatic tumor ferroptosis in mice, Science 368 (6486) (2020) 85–89.
[17] H. Miess, B. Dankworth, A.M. Gouw, M. Rosenfeldt, W. Schmitz, M. Jiang, et al., The glutathione redox system is essential to prevent ferroptosis caused by impaired lipid metabolism in clear cell renal cell carcinoma, Oncogene 37 (40) (2018) 5435–5450.
[18] W.S. Yang, R. SriRamaratnam, M.E. Welsch, K. Shimada, R. Skouta, V.S. Viswanathan, et al., Regulation of ferroptotic cancer cell death by GPX4, Cell 156 (1–2) (2014) 317–331.
[19] R Birsen, C Larrue, J Decroocq, N Johnson, N Guiraud, M Gotanegre, L Cantero-Aguilar, E Grignano, T Huynh, M Fontenay, O Kosmider, P Mayeux, N Chapuis, JE Sarry, J Tamburini, D Bouscary, APR-246 induces early cell death by ferroptosis in acute myeloid leukemia. Haematologica 107 (2) (2022) 403–416.
[20] Y. Du, J. Bao, M.J. Zhang, L.L. Li, X.L. Xu, H. Chen, et al., Targeting ferroptosis contributes to ATPR-induced AML differentiation via ROS-autophagy-lysosomal pathway, Gene 755 (2020) 144889.
[21] H.Y. Zhu, Z.X. Huang, G.Q. Chen, F. Sheng, Y.S. Zheng, Typhaneoside prevents acute myeloid leukemia (AML) through suppressing proliferation and inducing ferroptosis associated with autophagy, Biochem. Biophys. Res. Commun. 516 (4) (2019) 1265–1271.
[22] W. Wang, M. Green, J.E. Choi, M. Gijon, P.D. Kennedy, J.K. Johnson, et al., CD8(+) T cells regulate tumour ferroptosis during cancer immunotherapy, Nature 569 (7755) (2019) 270–274.
[23] Z. Zheng, X. Hong, X. Huang, X. Jiang, H. Jiang, Y. Huang, et al., Comprehensive analysis of ferroptosis-related gene signatures as a potential therapeutic target for acute myeloid leukemia: a bioinformatics analysis and experimental verification, Front. Oncol. 12 (2022) 930654.
[24] Z. Yin, F. Li, Q. Zhou, J. Zhu, Z. Liu, J. Huang, et al., A ferroptosis-related gene signature and immune infiltration patterns predict the overall survival in acute myeloid leukemia patients, Front. Mol. Biosci. 9 (2022) 959738.
[25] X. Huang, D. Zhou, X. Ye, J. Jin, A novel ferroptosis-related gene signature can predict prognosis and influence immune microenvironment in acute myeloid leukemia, Bosn. J. Basic Med. Sci. 22 (4) (2022) 608–628.
[26] Z. Cui, Y. Fu, Z. Yang, Z. Gao, H. Feng, M. Zhou, et al., Comprehensive analysis of a ferroptosis pattern and associated prognostic signature in acute myeloid leukemia, Front. Pharmacol. 13 (2022) 866325.
[27] Z. Zheng, W. Wu, Z. Lin, S. Liu, Q. Chen, X. Jiang, et al., Identification of seven novel ferroptosis-related long non-coding RNA signatures as a diagnostic biomarker for acute myeloid leukemia, BMC Med. Genom. 14 (1) (2021) 236.
[28] J.T. Leek, W.E. Johnson, H.S. Parker, A.E. Jaffe, J.D. Storey, The sva package for removing batch effects and other unwanted variation in high-throughput experiments, Bioinformatics 28 (6) (2012) 882–883.
[29] N. Zhou, Bao J. FerrDb, A manually curated resource for regulators and markers of ferroptosis and ferroptosis-disease associations, Database (2020) 2020.
[30] S.I. Vrieze, Model selection and psychological theory: a discussion of the differences between the Akaike information criterion (AIC) and the Bayesian information criterion (BIC), Psychol. Methods 17 (2) (2012) 228–243.
[31] M.E. Ritchie, B. Phipson, D. Wu, Y. Hu, C.W. Law, W. Shi, et al., Limma powers differential expression analyses for RNA-sequencing and microarray studies, Nucleic Acids Res. 43 (7) (2015) e47.
[32] G. Yu, L.G. Wang, Y. Han, Q.Y. He, clusterProfiler: an R package for comparing biological themes among gene clusters, OMICS 16 (5) (2012) 284–287.
[33] A. Liberzon, C. Birger, H. Thorvaldsdottir, M. Ghandi, J.P. Mesirov, P. Tamayo, The Molecular Signatures Database (MSigDB) hallmark gene set collection, Cell Syst 1 (6) (2015) 417–425.
[34] A.M. Newman, C.B. Steen, C.L. Liu, A.J. Gentles, A.A. Chaudhuri, F. Scherer, et al., Determining cell type abundance and expression from bulk tissues with digital cytometry, Nat. Biotechnol. 37 (7) (2019) 773–782.
[35] Z. Zhang, M.W. Kattan, Drawing Nomograms with R: applications to categorical outcome and survival data, Ann. Transl. Med. 5 (10) (2017) 211.
[36] A.C. Alba, T. Agoritsas, M. Walsh, S. Hanna, A. Iorio, P.J. Devereaux, et al., Discrimination and calibration of clinical prediction models: users' guides to the medical literature, JAMA 318 (14) (2017) 1377–1384.
[37] P. Geeleher, N. Cox, R.S. Huang, pRRophetic: an R package for prediction of clinical chemotherapeutic response from tumor gene expression levels, PLoS One 9 (9) (2014) e107468.
[38] W. Yang, J. Soares, P. Greninger, E.J. Edelman, H. Lightfoot, S. Forbes, et al., Genomics of Drug Sensitivity in Cancer (GDSC): a resource for therapeutic biomarker discovery in cancer cells, Nucleic Acids Res. 41 (Database issue) (2013) D955–D961.
[39] T.M. Garcia-Bates, G.M. Lehmann, P.J. Simpson-Haidaris, S.H. Bernstein, P.J. Sime, R.P. Phipps, Role of peroxisome proliferator-activated receptor gamma and its ligands in the treatment of hematological malignancies, PPAR Res. 2008 (2008) 834612.
[40] Y. Saito, R.H. Chapple, A. Lin, A. Kitano, D. Nakada, AMPK protects leukemia-initiating cells in myeloid leukemias from metabolic stress in the bone marrow, Cell Stem Cell 17 (5) (2015) 585–596.
[41] B.A. Carneiro, J.B. Kaplan, J.K. Altman, F.J. Giles, L.C. Platanias, Targeting mTOR signaling pathways and related negative feedback loops for the treatment of acute myeloid leukemia, Cancer Biol. Ther. 16 (5) (2015) 648–656.
[42] S. Piya, M. Andreeff, G. Borthakur, Targeting autophagy to overcome chemoresistance in acute myleogenous leukemia, Autophagy 13 (1) (2017) 214–215.
[43] D. Fu, B. Zhang, S. Wu, Y. Zhang, J. Xie, W. Ning, et al., Prognosis and characterization of immune microenvironment in acute myeloid leukemia through identification of an autophagy-related signature, Front. Immunol. 12 (2021) 695865.
[44] S. Huang, B. Zhang, W. Fan, Q. Zhao, L. Yang, W. Xin, et al., Identification of prognostic genes in the acute myeloid leukemia microenvironment, Aging (Albany NY) 11 (22) (2019) 10557–10580.
[45] S. Miyake, S. Murai, S. Kakuta, Y. Uchiyama, H. Nakano, Identification of the hallmarks of necroptosis and ferroptosis by transmission electron microscopy, Biochem. Biophys. Res. Commun. 527 (3) (2020) 839–844.
[46] Z. Lin, J. Liu, R. Kang, M. Yang, D. Tang, Lipid metabolism in ferroptosis, Adv Biol (Weinh). 5 (8) (2021) e2100396.
[47] Y. Zhao, C. Niu, J. Cui, Gamma-delta (gammadelta) T cells: friend or foe in cancer development? J. Transl. Med. 16 (1) (2018) 3.

[48] P. Qu, L.Z. Wang, P.C. Lin, Expansion and functions of myeloid-derived suppressor cells in the tumor microenvironment, Cancer Lett. 380 (1) (2016) 253–256.
[49] M.J. Szczepanski, M. Szajnik, M. Czystowska, M. Mandapathil, L. Strauss, A. Welsh, et al., Increased frequency and suppression by regulatory T cells in patients with acute myelogenous leukemia, Clin. Cancer Res. 15 (10) (2009) 3325–3332.
[50] J.C. Petrov, M. Wada, K.G. Pinz, L.E. Yan, K.H. Chen, X. Shuai, et al., Compound CAR T-cells as a double-pronged approach for treating acute myeloid leukemia, Leukemia 32 (6) (2018) 1317–1326.
[51] A. Ehninger, M. Kramer, C. Rollig, C. Thiede, M. Bornhauser, M. von Bonin, et al., Distribution and levels of cell surface expression of CD33 and CD123 in acute myeloid leukemia, Blood Cancer J. 4 (2014) e218.
[52] I. Pizzitola, F. Anjos-Afonso, K. Rouault-Pierre, F. Lassailly, S. Tettamanti, O. Spinelli, et al., Chimeric antigen receptors against CD33/CD123 antigens efficiently target primary acute myeloid leukemia cells in vivo, Leukemia 28 (8) (2014) 1596–1605.
[53] C.R. Ferrone, M.W. Kattan, J.S. Tomlinson, S.P. Thayer, M.F. Brennan, A.L. Warshaw, Validation of a postresection pancreatic adenocarcinoma nomogram for disease-specific survival, J. Clin. Oncol. 23 (30) (2005) 7529–7535.
[54] A. Bazarbachi, M. Labopin, G. Battipaglia, A. Djabali, J. Passweg, G. Socie, et al., Sorafenib improves survival of FLT3-mutated acute myeloid leukemia in relapse after allogeneic stem cell transplantation: a report of the EBMT Acute Leukemia Working Party, Haematologica 104 (9) (2019) e398–e401.
[55] I.N. Hahntow, F. Schneller, M. Oelsner, K. Weick, I. Ringshausen, F. Fend, et al., Cyclin-dependent kinase inhibitor Roscovitine induces apoptosis in chronic lymphocytic leukemia cells, Leukemia 18 (4) (2004) 747–755.
[56] X. Chen, R. Kang, G. Kroemer, D. Tang, Broadening horizons: the role of ferroptosis in cancer, Nat. Rev. Clin. Oncol. 18 (5) (2021) 280–296.
[57] M.S. D'Arcy, Cell death: a review of the major forms of apoptosis, necrosis and autophagy, Cell Biol. Int. 43 (6) (2019) 582–592.
[58] S. Zuo, J. Yu, H. Pan, L. Lu, Novel insights on targeting ferroptosis in cancer therapy, Biomark. Res. 8 (2020) 50.
[59] A. Ghoochani, E.C. Hsu, M. Aslan, M.A. Rice, H.M. Nguyen, J.D. Brooks, et al., Ferroptosis inducers are a novel therapeutic approach for advanced prostate cancer, Cancer Res. 81 (6) (2021) 1583–1594.
[60] D. Fu, B. Zhang, S. Wu, J. Feng, H. Jiang, Molecular subtyping of acute myeloid leukemia through ferroptosis signatures predicts prognosis and deciphers the immune microenvironment, Front. Cell Dev. Biol. 11 (2023) 1207642.
[61] M. Gao, P. Monian, Q. Pan, W. Zhang, J. Xiang, X. Jiang, Ferroptosis is an autophagic cell death process, Cell Res. 26 (9) (2016) 1021–1032.
[62] Y. Togashi, K. Shitara, H. Nishikawa, Regulatory T cells in cancer immunosuppression - implications for anticancer therapy, Nat. Rev. Clin. Oncol. 16 (6) (2019) 356–371.
[63] F. Yu, S. Sharma, J. Edwards, L. Feigenbaum, J. Zhu, Dynamic expression of transcription factors T-bet and GATA-3 by regulatory T cells maintains immunotolerance, Nat. Immunol. 16 (2) (2015) 197–206.
[64] C. Xu, S. Sun, T. Johnson, R. Qi, S. Zhang, J. Zhang, et al., The glutathione peroxidase Gpx4 prevents lipid peroxidation and ferroptosis to sustain Treg cell activation and suppression of antitumor immunity, Cell Rep. 35 (11) (2021) 109235.
[65] B. Silva-Santos, Promoting angiogenesis within the tumor microenvironment: the secret life of murine lymphoid IL-17-producing gammadelta T cells, Eur. J. Immunol. 40 (7) (2010) 1873–1876.
[66] S. Paul, G. Lal, Regulatory and effector functions of gamma-delta (gammadelta) T cells and their therapeutic potential in adoptive cellular therapy for cancer, Int. J. Cancer 139 (5) (2016) 976–985.
[67] M.Z. Koontz, S.J. Horning, R. Balise, P.L. Greenberg, S.A. Rosenberg, R.T. Hoppe, et al., Risk of therapy-related secondary leukemia in Hodgkin lymphoma: the Stanford University experience over three generations of clinical trials, J. Clin. Oncol. 31 (5) (2013) 592–598.
[68] R.E. Smith, J. Bryant, A. DeCillis, S. Anderson, B. National Surgical Adjuvant, E. Bowel Project, Acute myeloid leukemia and myelodysplastic syndrome after doxorubicin-cyclophosphamide adjuvant therapy for operable breast cancer: the National Surgical Adjuvant Breast and Bowel Project Experience, J. Clin. Oncol. 21 (7) (2003) 1195–1204.